Published by JScE as Proceedings of 4th International Conference on Role of Energy on Sustainable Social Development (RESSD-2025), 29-30 May, 2025, Kathmandu, Nepal

MATHEMATICAL MODELING AND ANALYSIS OF AN INVERTER-BASED RESOURCE

Avinash Karn[1]*, Shreeshuva Maharjan[1], Supriya Pandeya[1], Samundra Gurung[1], Diwakar Bista[1]

[1] Department of Electrical and Electronics Engineering, KU

Abstract

The transition from traditional synchronous machines to inverter-based resources is evident due to their ability to integrate renewable energy sources. Problems of instability due to the dynamics of the inverter, which is a major component of an Inverter-Based Resource (IBR), need to be modeled accordingly to stabilize the system behavior. This paper includes the development of a linearized state space model for a three-phase standalone inverter equipped with an LCL filter and RL load comprising IBR. A detailed mathematical framework in MATLAB, which includes a system of differential equations, state matrices ($\mathbf{A}$, $\mathbf{B}$, and $\mathbf{C}$), and eigenvalue analysis for stability assessment of the small-signal behavior of the inverter system, has been developed. The result includes the identification of critical modes and their participating states that provide insights into system nonlinearity and stability. All eight eigenvalues have real parts lying in negative real axis, with two of the modes having damping ratio 0.24% and 0.25% suggesting critically with frequency of oscillation of 3.69 kHz and 3.59 kHz, respectively. The model's efficacy to capture electromagnetic dynamics depicting two of the electromagnetic modes with a high frequency of oscillation around the resonance frequency has been presented, alongside a solid foundation for future feedback controller design in enhancing IBRs stability in renewable integration.

Keywords: Inverter-based resource, Nonlinear system, State space model, Linearization, Eigenvalue

1. Introduction

Innovations in small-scale distributed power generation systems combined with technological advancements in power electronic systems has led to concepts of future network technologies, such as, microgrids, and even comprises our conventional grid dominated by synchronous generation (Lasseter, 2002). These sources are asynchronous in nature and constitute of inverters, one of the major component of inverter-based resource (IBR) that are responsible for dc-ac power conversion and require proper models of inverter circuit and controllers for study and analysis. The IBRs are an emerging concept, that act in-accordance with the power electronic converters (PECs) in grid-connected and standalone applications. IBRs constitute of numerous renewable energy-based generations, that involve clean technologies like, photovoltaics, fuel-cell, battery energy storage, wind energy conversion system, etc. IBRs can offer increased reliability and efficiency, and can help integrate renewable energy and other forms of distributed generation (Lasseter, 2002). Employment of inverter provides the interface for new energy grid and the device to improve the power quality. Inverter is a critical component of the asynchronous system, which provides simplicity in design, higher power utilization rate, and efficient AC power attainment. The output voltage of inverter has reduced steady-state error, quicker dynamic response, and strong robustness to the network. The accuracy of results depend upon the main inverter circuit model and the rationality of control system (Wu et al., 2023).

Accurate mathematical models of inverters for the various loading condition considering the nonlinearities owing to switching, PWM, and saturation in the voltage and current is of prime concern. The analytical modeling method is helpful in analyzing the system behavior by constructing analytic expressions, unlike the digital simulation method, which uses various algorithms for numerical solutions. The simulation results are simple and intuitive, the physical model is understandable, and the calculation speed is

*Corresponding author: Avinash Karn
Department of Electrical and Electronics Engineering, Kathmandu University
Email: avinash5323@student.ku.edu.np
https://doi.org/10.3126/jsce.v12i2.91415

faster (Wu et al., 2023). State space models exhibit exceptional nonlinear prediction performance, maintaining extremely high accuracy with minimal parameter space, and effectively capturing the nonlinear features of the system (Wang et al., 2025). State space averaging to develop a model of a three-phase inverter operating with a nonlinear load has been proposed in (Wu et al., 2023). The model for the inverter with a nonlinear load is derived using linearization approximation and Laplace transformation for the small-signal state equation of the inverter under linear load, which was formulated using state-space averaging. MATLAB simulation of the model under both linear and nonlinear loads is performed and confirmed with an experimental setup for practicality and efficacy. In (Pogaku et al., 2007), modeling and analysis of the autonomous operation of IBR-based microgrid have been done, where the state-space form of all the components is obtained and combined in a common reference frame. The entire model is linearized around the operating point to obtain the resulting system matrix in order to derive the eigenvalues (or modes) and perform sensitivity analysis. The modes indicate frequency and damping of the transient response oscillatory component, while the sensitivity analysis identifies the origin of each mode to assist in designing the controllers for system stability improvement.

In the work presented in (Dozein et al., 2022), the mathematical analysis to study IBR dynamics in weak distribution have been investigated for converter control to understand disturbance performance characteristics of IBRs in a weak distribution feeder.

The paper (Poudel et al., 2023) demonstrates the development of a mathematical linearized state space model for parallel-connected Voltage Source Inverters (VSIs) to study their small signal stability. The model is integrated with feedback control based on parameter sensitivity of affecting states as the controller, load, and system parameters affect the small signal stability of the system.

While the research in (Li et al., 2023) develops a state space model for a generic power system with state-of-the-art inverters incorporating control system dynamics to investigate potential inverter-driven instability for the IEEE 39-bus system framework with a large-scale power system, this paper distinctly focuses on the small-signal stability of a standalone three-phase inverter with LCL filter and an RL load. This work distinguishes itself in the detailed modeling of the inverter-filter load configuration for system stability analysis.

Problems associated with stability, power sharing, and other interconnection issues of IBRs are resolved by developing models to imitate the inertial behavior of a synchronous machine and its controls, like the governor and exciter, in understanding the dynamics and control of IBRs. Inverter, filter, and load are collectively modeled as a state space model in the time domain for various time responses alike the classical power grid modeling. Thus, the small signal state space model of the IBRs is inherent to appraise the behavior of IBR to the small signal perturbations (Li et al., 2023; Pogaku et al., 2007).

The design of commercial inverters is proprietary or black box models based upon the performance specifications in the draft IEEE P2800 standard (Association et al., 2022). Owing to the importance of integration of IBRs into the network and the growing complexities in controller design, the control and design of generic models for inverter, not constrained to OEM's control or design specifications, becomes inherently important. The filter parameters constituting the inverters are not disclosed by the manufacturers. Neither any information about the filter resonance characteristics is explicitly mentioned except the maximum THD value. This can be challenging when we need to work at system levels. The explicit feature of these generic models provides ease of configuration for IBR design and control, which has been attempted as the preliminary open-loop model in this paper. By considering the importance of the inverter circuit in IBRs constituted modern power network, this study contributes to open loop modeling of standalone inverter circuit with LCL filter and load and modal analysis of the system stability.

The remainder of the paper is structured as follows: Section 2 discusses the inverter system configuration to follow the modeling. Section 3 establishes the switching average models of a three-phase inverter under load using the state-space averaging method with linearization around the steady state operating point. Section 4 illustrates the entire design parameter considerations. Section 5 demonstrates the theoretical analysis via simulation results. Section 6 investigates the state space matrices (A, B, and C) of the system and focuses on sensitivity analysis performance. Section 7 presents the conclusion about the model and eigenvalue analysis for controller design, suggesting future scope of work in the model.

2. System Description

To understand the system behavior pertaining to the system dynamics, the determination of $\mathbf{A}$, $\mathbf{B}$, and $\mathbf{C}$ matrices in open loop has been executed. Furthermore, to account for the system stability, the eigenvalues of the system have been attained and analyzed from the $\mathbf{A}$ matrix and step response of the system.

From Figure 1, we can see that the state of the system is fed to attain the differential state, i.e., the time state of the system, with the help of the state matrix ($\mathbf{A}$), which correlates the state of the system to its time state. The input matrix ($\mathbf{B}$) correlates the time state of the system to the external agency, which acts upon the system. The state

matrix is responsible for the free response of the system state, while the input matrix is responsible for the forced response of the system state.

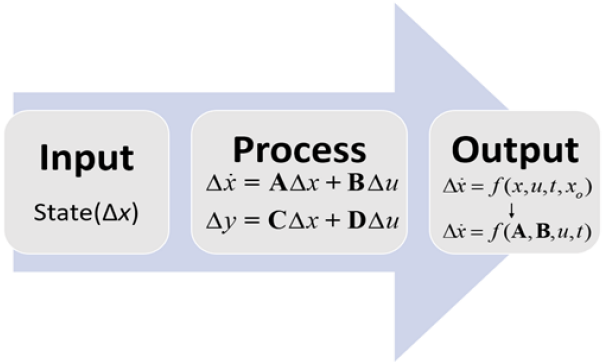

Figure 1. Process diagram of the system under consideration.

A three-phase inverter with LCL filter having a balanced RL load per phase is taken into consideration, as shown in Figure 2 to obtain a small signal linearized state space model around a steady operating point.

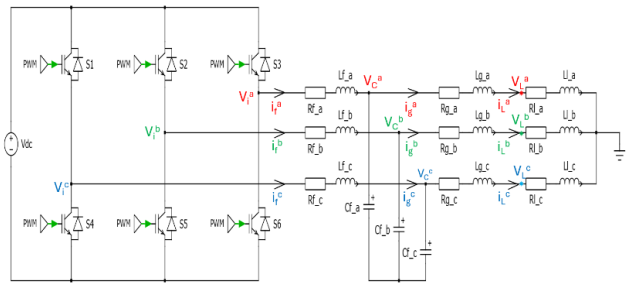

Figure 2. Circuit diagram of a three-phase inverter having LCL filter and RL load.

3. Linearized Small Signal State Space Model

3.1. System Variables

The key variables in the system are the inputs, states, outputs, and the system parameters. The duty cycles d_a, d_b, d_c, or the equivalent modulation signals V_i^a, V_i^b, Vi_c being the function of duty cycles, can be taken as inputs. The inverter side filter inductor currents (i_f^a, i_f^b, i_f^c), the filter capacitor voltages (V_C^a , V_C^b, V_C^c), the load side filter inductor currents (i_g^a, i_g^b, i_g^c), and the load currents (i_L^a, i_L^b, i_L^c) are the state vectors. The load voltages (V_L^a, V_L^b, V_L^c) are the output, or the load currents can be the output, depending upon our control objective. The system parameters include DC-link voltage (V_{dc}), the inverter side filter inductance with parasitic resistance (L_f, R_f), the filter capacitance (C_f), the grid side filter inductance with parasitic resistance (L_g, R_g), and the load resistance and inductance (R_l, L_l) for each phase.

3.2. Nonlinear Dynamic Equations per Phase

For the system dynamics, a Y-connected balanced load with a neutral point is assumed. The nonlinear differential equations for each phase (say, for phase "a") and the dynamics offered by components can be described as in Equation (1).

$$\begin{bmatrix} \dot{i_{fa}} \\ \dot{V_{Ca}} \\ \dot{i_{ga}} \\ \dot{i_{La}} \end{bmatrix} = \frac{d}{dt}\begin{bmatrix} i_{fa} \\ V_{Ca} \\ i_{ga} \\ i_{La} \end{bmatrix} = \begin{bmatrix} \frac{1}{L_f}(V_{ia} - R_f i_f - V_{Ca}) \\ \frac{1}{C_f}(i_{fa} - i_{ga}) \\ \frac{1}{L_g}(V_{Ca} - R_g i_g - V_{La}) \\ \frac{1}{L_l}(V_{Ca} - R_g i_g - R_l i_{La}) \end{bmatrix} \tag{1}$$

Similar nonlinear differential equations for the other two phases (phase "b" and phase "c") can be illustrated for full dynamics of the system.

3.3. Dynamic Equations in dq-frame

Park's transformation is a tool for transforming three-phase variables to DC components, i.e., rectangular components, one along the direct-axis and the other along the quadrature-axis, by rotating electrical quantities synchronously with the network frequency. This is the most common method to find the linear time invariant (LTI) model of a time-varying system (here, phases "a", "b", "c" being time variant).

The full nonlinear state space model is given as in Equation (3) on the basis of the analytical in Equation (2) (Friedland, 2005):

$$\dot{x} = f(x, u, t) \tag{2}$$

where,

State vector: $x = [i_{fd}, i_{fq}, V_{Cd}, V_{Cq}, i_{gd}, i_{gq}, i_{Ld}, i_{Lq}]^T$

Input vector: $u = [V_{id}, V_{iq}]^T$

Following Equation (2), we get arrive at Equation (3), as follows:

$$\begin{bmatrix} \dot{i_{fd}} \\ \dot{i_{fq}} \\ \dot{V_{Cd}} \\ \dot{V_{Cq}} \\ \dot{i_{gd}} \\ \dot{i_{gq}} \\ \dot{i_{Ld}} \\ \dot{i_{Lq}} \end{bmatrix} = \frac{d}{dt}\begin{bmatrix} i_{fd} \\ i_{fq} \\ V_{Cd} \\ V_{Cq} \\ i_{gd} \\ i_{gq} \\ i_{Ld} \\ i_{Lq} \end{bmatrix} = \begin{bmatrix} \frac{1}{L_f}(V_{id} - R_f i_{fd} + \omega L_f i_{fq} - V_{Cd}) \\ \frac{1}{L_f}(V_{iq} - R_f i_{fq} - \omega L_f i_{fd} - V_{Cq}) \\ \frac{1}{C_f}(i_{fd} - i_{ld} + \omega C_f V_{Cq}) \\ \frac{1}{C_f}(i_{fq} - i_{lq} + \omega C_f V_{Cd}) \\ \frac{1}{L_g}(V_{Cd} - R_g i_{gd} + \omega L_g i_{gq} - V_{Ld}) \\ \frac{1}{L_g}(V_{Cq} - R_g i_{gq} - \omega L_g i_{gd} - V_{Lq}) \\ \frac{1}{L_l}(V_{Cd} - R_g i_{gd} - \omega L_g i_{gq} - R_l i_{ld}) \\ \frac{1}{L_l}(V_{Cq} - R_g i_{gq} - \omega L_g i_{gd} - R_l i_{lq}) \end{bmatrix} \tag{3}$$

3.4. Linearized Small Signal State Space Equations

The state space equation for a dynamical system having x state vector and u input vector can be illustrated as in Equation (4).

$$\dot{x} = f(x, u, t) = \mathbf{A}x + \mathbf{B}u \tag{4}$$

where, $\mathbf{A}$ is state matrix and $\mathbf{B}$ is input matrix linearized along (x_o, u_o) operating point.

For the dynamic system expressed in Equation (4), linearized small signal state space equation is obtained by expanding Equation (4) by taking infinitesimally small increment in the neighborhood around an operating point (x_o, u_o), is as depicted in Equation (5):

$$\dot{x} + \Delta\dot{x} = f(x + \Delta x, u + \Delta u, t)$$

$$\dot{x}+\Delta\dot{x} = f(x)+\sum_{n=1}^{\infty}\frac{d^n f}{dx^n}\bigg|_{x_o}\Delta x^n+f(u)+\sum_{m=1}^{\infty}\frac{d^m f}{du^m}\bigg|_{u_o}\Delta u^m \quad (5)$$

From Taylor series expansion, taking only the first order differentiation, as this is only the most significant in the linear expansion of Equation (5), which can be rewritten as shown in Equation (6):

$$\Delta\dot{x} = \frac{df}{dx}\bigg|_{x_o}\Delta x + \frac{df}{du}\bigg|_{u_o}\Delta u \quad (6)$$

Thus, the final linearized small-signal state space equation is obtained, which is shown in Equation (7):

$$\Delta\dot{x} = \mathbf{A}\Delta x + \mathbf{B}\Delta u \quad (7)$$

where, $\mathbf{A} = \frac{df}{dx}\Big|_{x_0}$, and $\mathbf{B} = \frac{df}{du}\Big|_{u_0}$

The final linearized small-signal state space model for our system can be written as in Equation (8), derived from Equation (3):

$$\begin{bmatrix}\Delta\dot{i}_{fd}\\ \Delta\dot{i}_{fq}\\ \Delta\dot{V}_{Cd}\\ \Delta\dot{V}_{Cq}\\ \Delta\dot{i}_{gd}\\ \Delta\dot{i}_{qq}\\ \Delta\dot{i}_{Ld}\\ \Delta\dot{i}_{Lq}\end{bmatrix} = \mathbf{A}\begin{bmatrix}\Delta i_{fd}\\ \Delta i_{fq}\\ \Delta V_{Cd}\\ \Delta V_{Cq}\\ \Delta i_{gd}\\ \Delta i_{gq}\\ \Delta i_{Ld}\\ \Delta i_{Lq}\end{bmatrix} + \mathbf{B}\begin{bmatrix}\Delta V_{id}\\ \Delta V_{iq}\end{bmatrix} \quad (8)$$

where,

State vector:

$\Delta x = [\Delta i_{fd}, \Delta i_{fq}, \Delta V_{Cd}, \Delta V_{Cq}, \Delta i_{gd}, \Delta i_{gq}, \Delta i_{Ld}, \Delta i_{Lq}]^T$

Input vector: $\Delta u = [\Delta V_{id}, \Delta V_{iq}]^T$

Similarly, the output vector taken as capacitor voltage in d and q-axes can be represented as in Equation (9):

$$\begin{bmatrix}\Delta V_{Cd}\\ \Delta V_{Cq}\end{bmatrix} = \mathbf{C}\begin{bmatrix}\Delta i_{fd}\\ \Delta i_{fq}\\ \Delta V_{Cd}\\ \Delta V_{Cq}\\ \Delta i_{gd}\\ \Delta i_{gq}\\ \Delta i_{Ld}\\ \Delta i_{Lq}\end{bmatrix} \quad (9)$$

where, y $= g(x)$, and $\mathbf{C} = \frac{dg}{dx}\Big|_{x_o}$.

For this purpose, the state space model is linearized along a steady state, such that,

$\Delta\dot{x_o} = [\Delta\dot{i}_{fd}, \Delta\dot{i}_{fq}, \Delta\dot{V}_{Cd}, \Delta\dot{V}_{Cq}, \Delta\dot{i}_{gd}, \Delta\dot{i}_{gq}, \Delta\dot{i}_{Ld}, \Delta\dot{i}_{Lq}]^T = 0$

Then from Equation (7), we get to Equation (10):

$$\Delta x_o = -\mathbf{A}^{-1}\mathbf{B}\Delta u_o \quad (10)$$

Here, from Equation (10), we finally arrive to Eqaution (11):

$$\Delta x_o = -\mathbf{A}^{-1}\mathbf{B}\begin{bmatrix}\Delta V_{ido}\\ \Delta V_{iqo}\end{bmatrix} \quad (11)$$

$$\mathbf{A} = \begin{bmatrix} -\frac{R_f}{L_f} & \omega & -\frac{1}{L_f} & 0 & 0 & 0 & 0 & 0 \\ -\omega & -\frac{Rf}{Lf} & 0 & -\frac{1}{L_f} & 0 & 0 & 0 & 0 \\ \frac{1}{C_f} & 0 & 0 & \omega & -\frac{1}{C_f} & 0 & 0 & 0 \\ 0 & \frac{1}{C_f} & -\omega & 0 & 0 & -\frac{1}{C_f} & 0 & 0 \\ 0 & 0 & \frac{1}{L_g} & 0 & -\frac{R_g}{L_g} & \omega & 0 & 0 \\ 0 & 0 & 0 & \frac{1}{L_g} & -\omega & -\frac{R_g}{L_g} & 0 & 0 \\ 0 & 0 & 0 & 0 & \frac{1}{L_l} & 0 & -\frac{R_l}{L_l} & \omega \\ 0 & 0 & 0 & 0 & 0 & \frac{1}{L_l} & -\omega & -\frac{R_l}{L_l} \end{bmatrix} \quad (12)$$

$$\mathbf{B} = \begin{bmatrix} \frac{1}{L_f} & 0 \\ 0 & \frac{1}{L_f} \\ 0 & 0 \\ 0 & 0 \\ 0 & 0 \\ 0 & 0 \\ 0 & 0 \\ 0 & 0 \end{bmatrix} \quad (13)$$

$$\mathbf{C} = \begin{bmatrix} 0 & 0 & 1 & 0 & 0 & 0 & 0 & 0 \\ 0 & 0 & 0 & 1 & 0 & 0 & 0 & 0 \end{bmatrix} \quad (14)$$

4. System Parameters

The inputs to the system can be categorized as the input in the inverter and the system parameters. The duty cycles d_a, d_b, d_c or the equivalent modulation signals obtained at the inverter output terminal as V_i^a, V_i^b, V_i^c, being the function of duty cycles, can be taken as inputs, which later are transformed into dq0 axes, i.e., V_{id} and V_{iq} are the inverter inputs. Additionally, the system parameters treated as inputs include DC-link voltage (V_{dc}), the inverter side filter inductance with parasitic resistance (L_f, R_f), the filter capacitance (C_f), the load side filter inductance with parasitic resistance (L_g, R_g), and the load resistance and inductance (R_l, L_l) for each phase. The entire system parameters have been enlisted in Table 1.

The DC side input voltage has been chosen as 800 V to attain 230 V phase rms voltage inverter output with

Table 1. System parameter settings

Parameters	**Value**
DC side input voltage (V_{dc})	800 V
Inverter side filter inductance (L_f)	2.56 mH
Inverter side filter resistance (R_f)	0.05 Ω
Filter capacitance (C_f)	5 μF
Load side filter inductance (L_g)	2.56 mH
Load side filter resistance (R_g)	0.05 Ω
Load resistance (R_l)	2 Ω
Load inductance (L_l)	5 mH
Synchronous frequency (f)	50 Hz
Switching frequency (f_s)	20 kHz
Resonant frequency (f_{res})	1.98 kHz

amplitude modulation (m_a) of 0.813. The active power output of the inverter is taken as 5 kW. High frequency modulation (m_f) with sinusoidal PWM gate switching frequency (f_s) of 20 kHz is taken. The calculations for L_g, C_f, and resonant frequency of oscillation (f_{res}) are provided in (Sarkar, 2015), and the respective Bode plot for the input-output behavior has been shown in Figure 3.

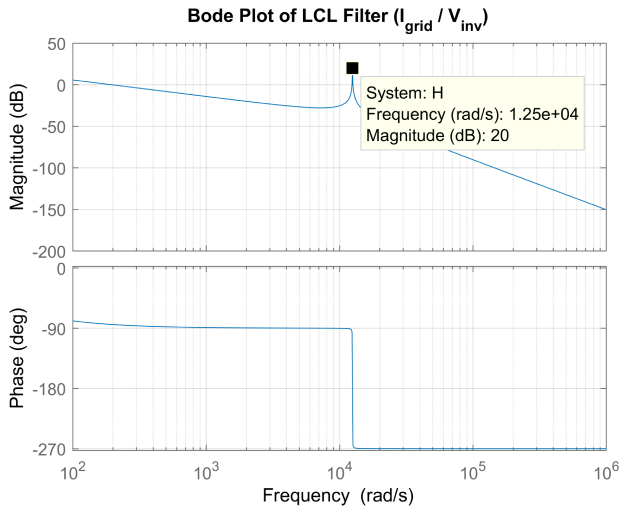

Figure 3. Bode plot of grid current to LCL filter input voltage.

5. Simulation Results

The proposed linearized small signal state space model for a three-phase inverter with LCL filter and load has been demonstrated in MATLAB. The work progresses with the determination of **A** and **B** matrices, which form the state space equation for the system. **A**, **B**, and **C** matrices has been obtained using Equation (12), Equation (13), and Equation (14) respectively.

For the state space model linearized along the steady state, such that the input vector $\Delta u = [\Delta V_{id}, \Delta V_{iq}]^T$. Here, the inputs are taken as ΔV_{ido} =10% of V_{dc}(=40 V) and ΔV_{iqo} =0 i.e. existing only along d-axis.

The step response of the system with a time step of 50μs, i.e. f_s = 20 kHz, is plotted attaining the steady state till 0.5 s as in Figure 4, Figure 5 and Figure 6 depicting both dq-frame and abc-frame plots. In Figure 7, the state variables associated with the currents have been plotted. Figure 8 illustrates eigenvalues obtained from the state transition matrix **A** for the model.

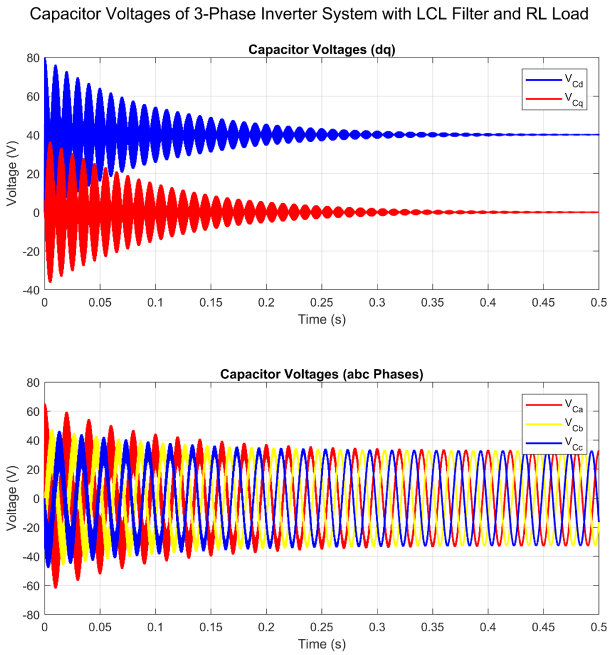

Figure 4. Capacitor voltage in dq and abc frames.

The eigenvalues with the corresponding real part and the imaginary part are encapsulated in Table 2. Here, eigen values $\lambda 1$ and $\lambda 2$ being complex conjugate pair constitutes mode 1, and, similarly, mode 2, mode 3 and mode 4 can be illustrated comprising $\lambda 3$ & $\lambda 4$, $\lambda 5$ & $\lambda 6$ and $\lambda 7$ & $\lambda 8$ respectively. The modes with their respective frequency of oscillation, damping ratio, and participating states are shown in Table 3.

6. Discussion

In this paper, from the step response i.e. linearizing around steady state with the initial state differentiation ($\Delta \dot{x}$) being zero, a significant distortion at the beginning for load voltage is evident from the plot in Figure 5, which is possible due to the transient response provided by the input signal (Δu). A similar response is seen

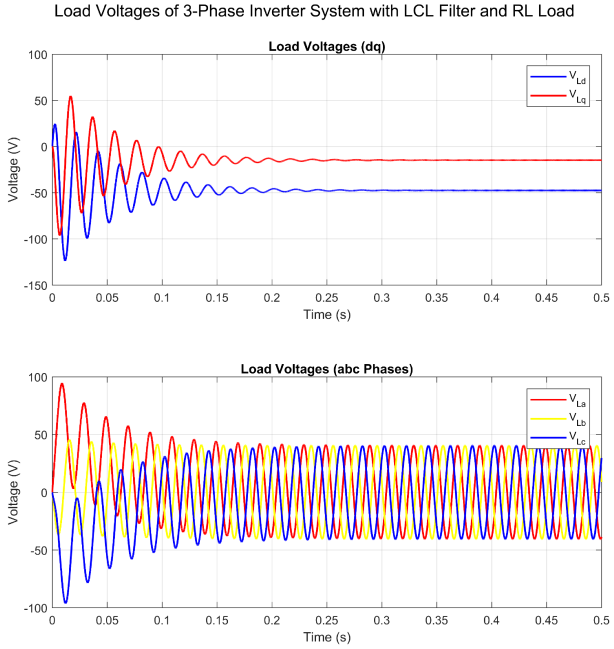

Figure 5. Load voltage in dq and abc frames

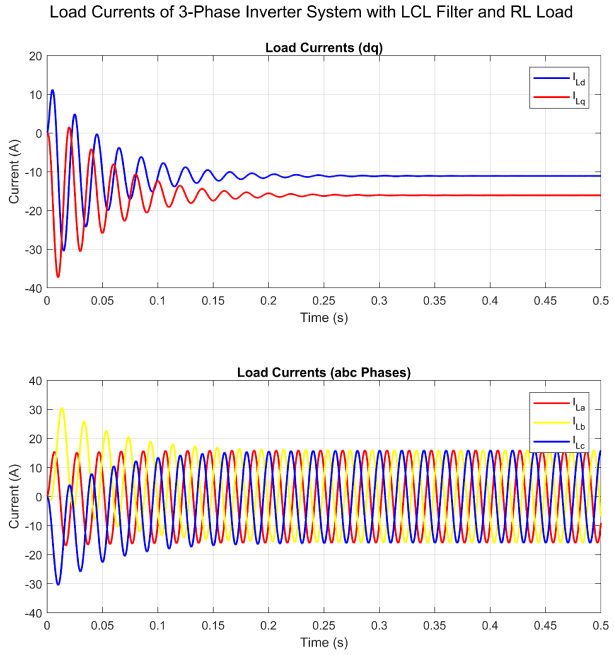

Figure 6. Load current in dq and abc frames

for the capacitor voltage and load current as dictated in Figure 4 and Figure 6 respectively, indicating the response as achieving a steady region after 0.4 s. The transient response can be studied further to attain information on maximum overshoot, peak time, rise time, settling time, etc., like dynamic characteristics, which are not greater interest. From Table 2 and Figure 8, all the eigenvalues

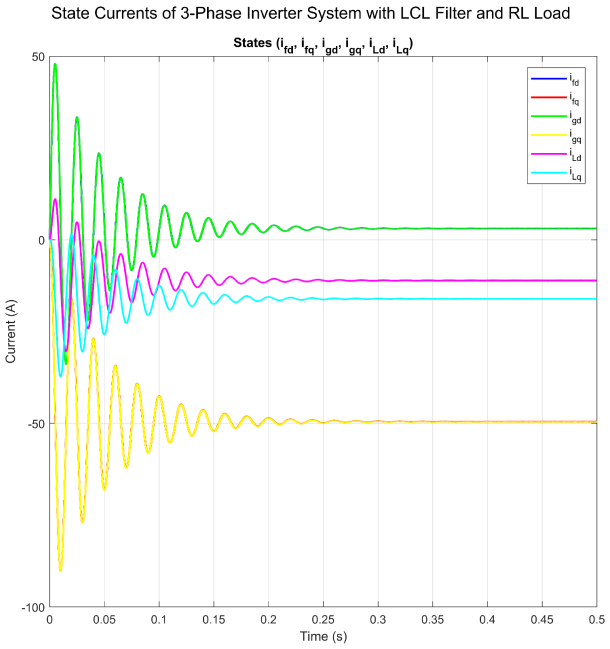

Figure 7. State currents in dq-frame

Table 2. Eigen values of the system

Eigen values	**Real part**	**Imaginary part**
$\lambda 1$	-10	j12814
$\lambda 2$	-10	-j12814
$\lambda 3$	-10	j12186
$\lambda 4$	-10	-j12186
$\lambda 5$	-20	j314
$\lambda 6$	-20	-j314
$\lambda 7$	-400	j314
$\lambda 8$	-400	-j314

lie in the left half plane (LHP), which indicates the system is stable. $\lambda 1$, $\lambda 2$, $\lambda 3$, $\lambda 4$, $\lambda 5$, and $\lambda 6$ have their real part close to zero, indicating that these poles have exponential decay with a larger time constant than those of $\lambda 7$ and $\lambda 8$. Also, the imaginary part for $\lambda 5$, $\lambda 6$, $\lambda 7$, and $\lambda 8$ have frequency of oscillation, $\omega = 314.15$ rad/s i.e., 50 Hz, indicating that these poles comprising of sinusoids vibrates at synchronous frequency of the system. Other poles, $\lambda 1$, $\lambda 2$, $\lambda 3$, and $\lambda 4$ have a much higher frequency of oscillation ($>>$ 50 Hz), indicating that these poles comprise non-synchronous sinusoids introduced due to the resonance frequency of oscillation of PWM, which are responsible for system nonlinearity.

From the sensitivity analysis of the system, as shown

in Table 3, mode 1 and mode 2 show a very high frequency of oscillation around $fres$, i.e., 1989.43 Hz and a very low damping ratio ($< 5\%$), suggesting that these are the critical modes of the system. These modes need to be investigated for controller tuning to improve the damping ratio, mitigation of nonlinearity, and acknowledging stability concerns in the system.
From the results in Figure 7, we can see that that i_{fd} & i_{gd},

Table 3. Modes and their characteristics

Modes	Frequency of oscillation (Hz)	Damping ratio (%)	Participating states
1	2039	0.078	i_f, i_g, V_C
2	1939	0.082	i_f, i_g, V_C
3	50	6.36	i_f, i_g
4	50	78.65	i_L

and i_{fq}, & i_{gq} follow the same trajectory, which indicate the current state in capacitor is of no purpose i.e., the only one current state, either i_f (or i_g) can be considered for reduced order modeling. Our system reduces in-state providing controllability of only two of the participating states for critical modes as depicted in Table 3, which provides less complexity in controller parameter tuning.

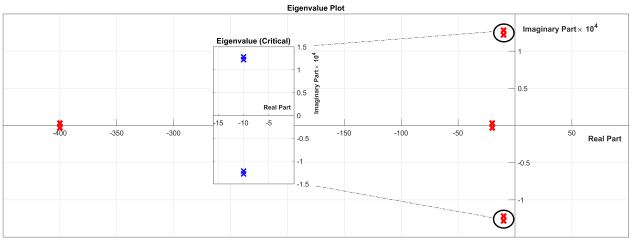

Figure 8. Eigen value plot

7. Conclusion

IBR inherently consists of nonlinear dynamics. The linearized small-signal state space model for three phase inverter with an LCL filter feeding an RL load can be implemented to understand the dynamics of the standalone IBR. The open-loop model of the system illustrated for linearization around the steady state operating point under consideration can be synthesized by the determination of $\mathbf{A}$ and $\mathbf{B}$ matrices of the state space model. The participating states, owing to critical modes, need to be considered for further controller design and stability analysis.
The LCL filter parameters are designed based on constraints like limits on power factor, THD, and the sizes of the passive elements, i.e., inductors and capacitors.
High-frequency ripple in voltages and currents in the inverter circuit is introduced by PWM, which is typically neglected in a linearized state space model because linearization assumes small-signal perturbations around a steady state operating point and focuses on low-frequency dynamics. This allows for a continuous, averaged steady-state space model.
Inclusion of various control strategies for feedback modeling enables shifting of the modes contributing to nonlinearity to the linear region and provides the system with improved controllability and response.

Acknowledgments

This work is supported by the Capacity Enhancement in Electrical Equipment Condition Monitoring and Fault Diagnostics (CEEECoM) project (Grant ID: 101082996).

References

Association, I. S., et al. (2022). Ieee standard for interconnection and interoperability of inverter-based resources (ibrs) interconnecting with associated transmission electric power systems. *IEEE Std*, 2800–2022.

Dozein, M. G., Pal, B. C., & Mancarella, P. (2022). Dynamics of inverter-based resources in weak distribution grids. *IEEE Transactions on Power Systems*, *37*(5), 3682–3692.

Friedland, B. (2005). *Control system design: An introduction to state-space methods*. Dover Publications.

Lasseter, R. H. (2002). Microgrids. *2002 IEEE power engineering society winter meeting. Conference proceedings (Cat. No. 02CH37309)*, *1*, 305–308.

Li, Y., Fu, L., Li, Q., Wang, W., Jia, Y., & Dong, Z. Y. (2023). Small-signal modelling and stability analysis of grid-following and grid-forming inverters dominated power system. *Global Energy Interconnection*, *6*(3), 363–374.

Pogaku, N., Prodanovic, M., & Green, T. C. (2007). Modeling, analysis and testing of autonomous operation of an inverter-based microgrid. *IEEE Transactions on power electronics*, *22*(2), 613–625.

Poudel, N., Shrestha, S., & Neupane, D. Small signal stability of parallel connected voltage source inverters. In: In *Proceeedings of 14th ioe graduate conference*. 2023.

Sarkar, A. (2015). *Modeling and control of a three phase voltage source inverter with an lcl filter* [Master's thesis, Arizona State University].

Wang, Q., Jin, Y., Lu, Z., Gao, Q., Ge, X., Li, Z., & Hou, L. (2025). State space model: A magical tool for

state prediction in nonlinear systems. *Nonlinear Dynamics*, *113*(7), 6577–6603.

Wu, F., Zhang, B., Meng, G., Chen, C., Yang, B., & Chen, B. (2023). State-space-based three-phase inverter modeling under nonlinear load. *2023 7th CAA International Conference on Vehicular Control and Intelligence (CVCI)*, 1–6.

This page is intentionally left blank.